

www.acsami.org Research Article

Injection Molding of Liquid Metal by Harnessing Nonstick Molds

Jinwoo Ma, Dhwanil P. Vaghani, Sooik Im, Minsik Kong, Mohammad Shamsi, Shuzhen Wei, Man Hou Vong, and Michael D. Dickey*



Cite This: ACS Appl. Mater. Interfaces 2024, 16, 10931–10941



ACCESS

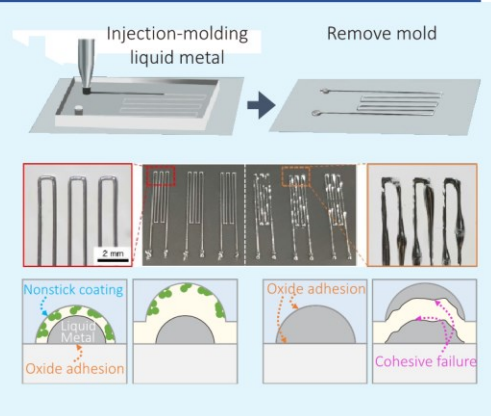




Article Recommendations

Supporting Information

ABSTRACT: The fluid nature of liquid metals combined with their ability to form a solid native oxide skin enables them to be patterned in ways that would be challenging for solid metals. The present work shows a unique way of patterning liquid metals by injecting liquid metals into a mold. The mold contains a nonstick coating that enables the removal of the mold, thereby leaving just the liquid metal on the target substrate. This approach offers the simplicity and structural control of molding but without having the mold become part of the device. Thus, the metal can be encapsulated with very soft polymers that collapse if used as microchannels. The same mold can be used multiple times for high-volume patterning of liquid metal. The injection molding method is rapid and reliably produces structures with complex geometries on both flat and curved surfaces. We demonstrate the method by fabricating an elastomeric Joule heater and an electroadhesive soft gripper to show the potential of the method for soft and stretchable devices.



KEYWORDS: liquid metal, injection molding, patterning, Joule heater, electroadhesion



INTRODUCTION

Liquid metals (LMs) are promising conductors for stretchable electronics, wearable devices, and soft robotics because LMs combine the high electrical conductivity of a metal with the deformability of a fluid. In particular, galliumbased liquid metals are attractive because of their low viscosity, low vapor pressure, and low toxicity.¹

Patterning of LMs is a critical step for their utilization for devices. The liquid nature of LM allows it to be patterned in some truly unique ways relative to conventional solid metals, such as injection into cavities and microchannels. Injecting LM is appealing because the metal can fill the cavities, thereby providing precise geometric control over the metal structures. We report here a process in which LM is injected into microchannels formed by placing a mold against a surface. After injection, removal of the mold leaves only LM features on the substrate. This process resembles injection molding, a commercial process that involves injecting molten plastic into a mold and then removing the mold after the part solidifies by cooling. Here, the injection is done entirely at room temperature; the solid native oxide layer^{3,4} that forms on the surface of the metal stabilizes the

molded LM part rather than phase change. Consequently, the injected parts are limited to dimensions below the capillary length (\approx mm) to ensure that they remain stable after injection. Unlike injection-molded plastic parts, which are sufficiently rigid to be handled, the injection-molded LM remains liquid and must have at least one surface adhered to a surface to facilitate handling. Therefore, in addition to stabilizing the patterned metal, the oxide layer must also adhere to the substrate. Fortunately, oxides adhere to nearly all surfaces, except those that are rough. The envisioned process should therefore use a mold with a rough coating to prevent oxide adhesion so that the metal parts remain adhered to the smooth substrate rather than the rough mold during demolding or lift-off.

One of the commercial appeals of injection molding is that it can rapidly fabricate plastic parts with excellent dimensional control.⁵ In addition to rapid fabrication, the ability to injection mold LM can be useful for (1) decoupling the materials used for molding and embedding of the LM, (2) patterning metal on curved surfaces, (3) depositing exposed LM structures on surfaces without encapsulation, or (4) making direct contact with exposed metal features after the mold. Regarding the first point, we note that it is challenging to directly inject liquid metal into microchannels

composed of ultrasoft materials, such as Ecoflex, because the channels tend to collapse. Instead, here any convenient mold material may be used to pattern the metal onto arbitrary substrates, and then after removing the mold, the patterned metal can be encased in a wide variety of materials (including silicones with low moduli such as Ecoflex, which can be used to create ultrasoft and stretchable conductors).

Received: November 13, 2023
Revised: January 25, 2024
Accepted: January 25, 2024
Published: February 20, 2024



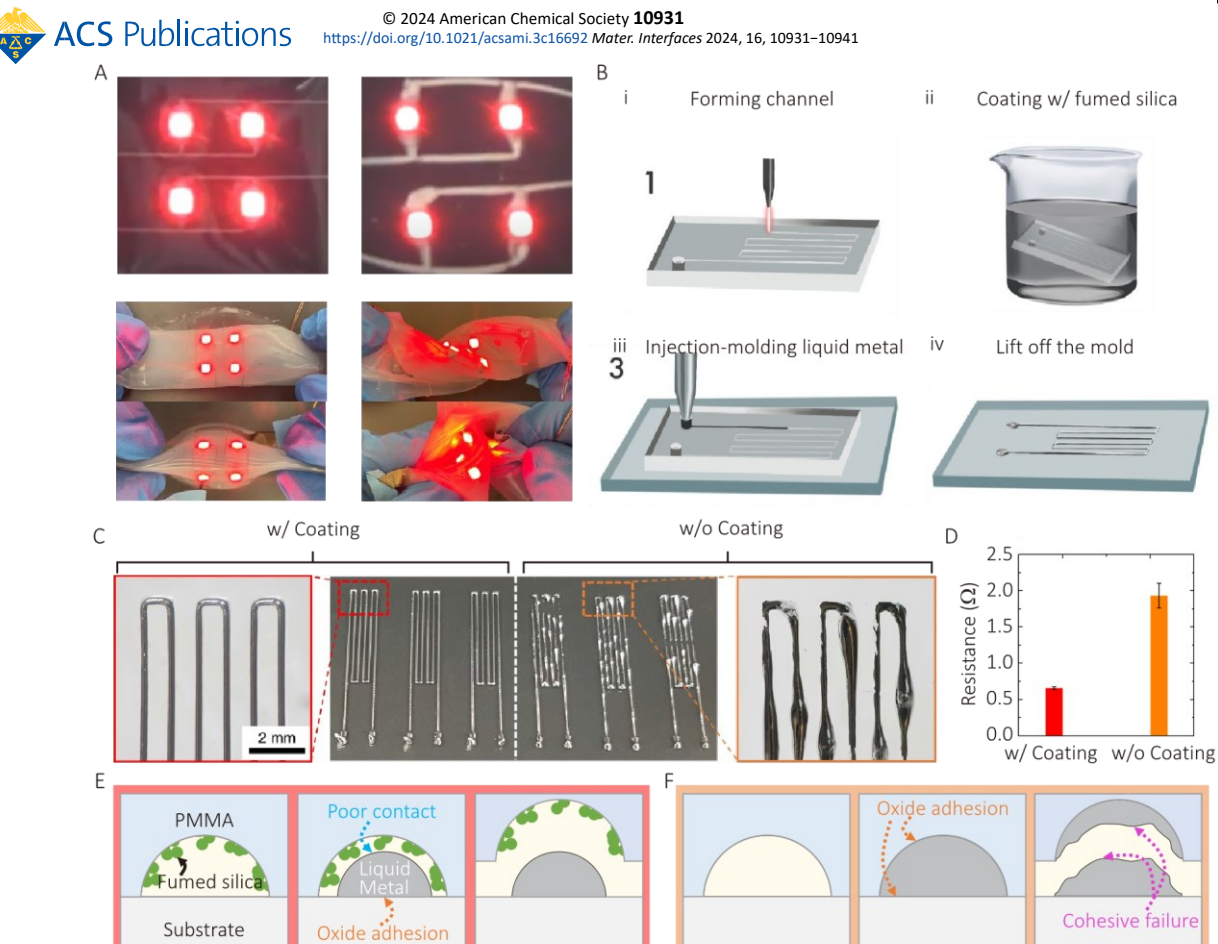


Figure 1. Patterning of liquid metal by injection molding, which utilizes a "nonstick" channel created by using a rough surface coating to prevent adhesion with the oxide-coated metal. (A) This method can produce a highly deformable 2 × 2 LED array embedded in a stretchable elastomer and wired using LM. (B) The method: (i) A microchannel, inlet, and outlet were generated on a thermoplastic by using laser engraving (SI Video 1). (ii) The thermoplastic was coated with fumed silica, thereby rendering the surface rough (SI Video 2). (iii) After placing the mold on a substrate, the liquid metal was injected to fill the microchannel (SI Video 3). (iv) The liquid metal patterns remain on the substrate after lifting off the mold (SI Video 3). (C) Comparison of the liquid metal patterns with and without the coating. The liquid metal pattern was uniform using a particlecoated mold, but the liquid metal pattern was damaged if the mold was uncoated. (D) The resistance of the liquid metal pattern with/without the coating. (E, F) Schematic cross section of the lift-off step (not to scale). The contact between the oxide on the liquid metal and the fumed silica is poor; therefore, the liquid metal does not adhere to the mold. The liquid metal cohesively fails if the mold is not coated, because of the adhesive nature of the oxide layer of the liquid metal.

Here, we report a method to pattern LM at submillimeter length scales by injection molding. Briefly, LM gets injected into a nonstick microchannel mold (i.e., no adhesion between LM and the microchannel) that rests temporarily on a target substrate. The LM does not stick to the walls of the mold due to a rough coating that resists adhesion to the

native oxide that forms on the surface of the LM. Thus, separating the mold from the substrates leaves the LM pattern on the substrate. In other words, the mold did not become part of the final device. The metal replicates the features of the mold ($\sim 100~\mu m$ width), the shapes are highly reproducible, and the process is facile enough for mass

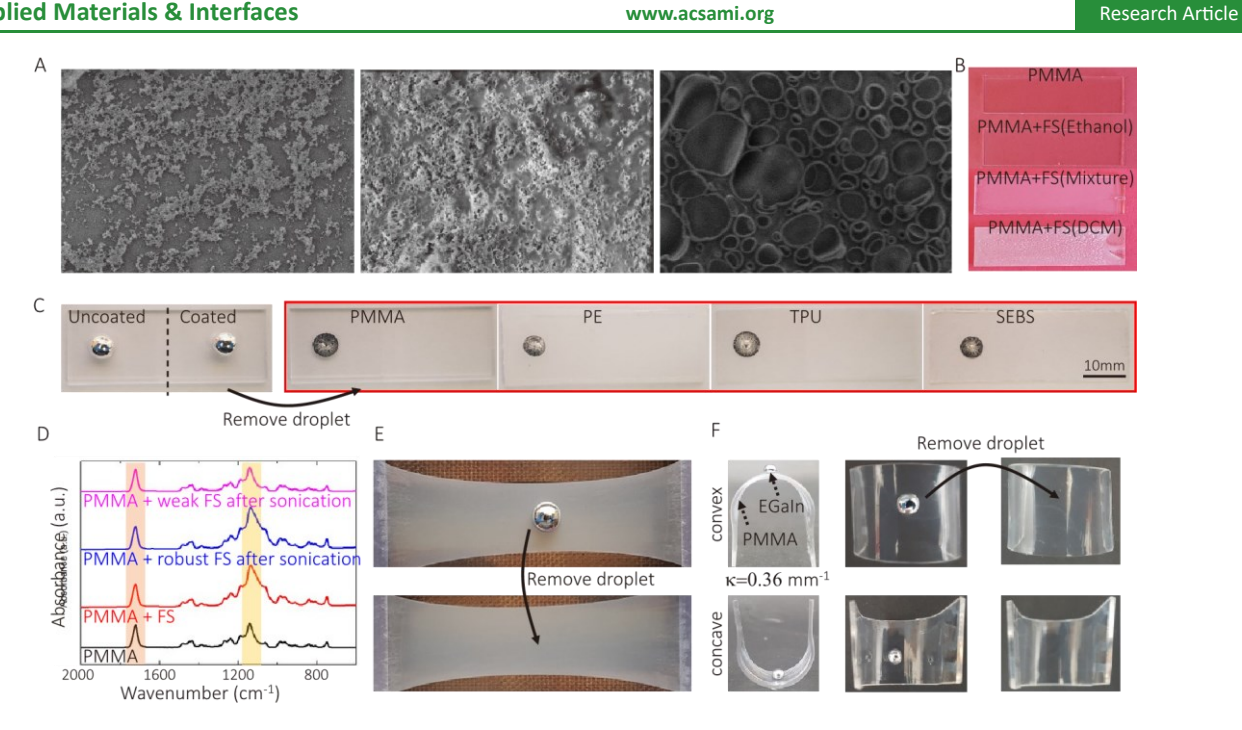


Figure 2. Characterization of the surface of nonstick substrates. (A) SEM images of weakly bound FS (left, right) and robustly bound FS (center) on PMMA achieved by using different solvents. (B) Optical images of PMMA with and without FS coating using various solvents. (C) Simple advancing and receding liquid metal experiments on the various FS-coated thermoplastics. The right-hand side of the substrate was coated with the FS and showed a nonadhesive nature to LM relative to the uncoated, left-handed side. (D) FT-IR spectra of the PMMA, the FS-coated PMMA, and the FS-coated PMMA after sonication. (E, F) Advancing and receding liquid metal experiments on stretched TPU (E) and thermoformed PMMA (F). During receding, the liquid metal is completely removed from the surface, which shows the poor adhesion on the treated surfaces.

production. We demonstrate two applications that use this technique for device fabrication: a soft, stretchable Joule heater and an electroadhesive soft gripper device.



RESULTS AND DISCUSSION

To demonstrate the utility of the injection molding technique, we fabricated a circuit with an array of LEDs connected by liquid metal in Ecoflex (Figure 1A). The LED array functions under all deformation modes, including stretching, rolling, folding, twisting, and crumpling. We created the mold from thermoplastic poly(methyl methacrylate) (PMMA) by using a commercial laser engraver (VLS 3.50, ULSsee the

Experimental Section for details) to locally ablate grooves in the surface or cut through-hole inlets and outlets for injection (Figure 1B-i). Using this laser cutter, the molds were limited to minimum sizes of $\sim 200 \,\mu\text{m}$, but in principle, the thermoplastic mold could be created by other methods (e.g., injection molding, milling, three-dimensional (3D) printing). 6-10 We coated the thermoplastic mold with fumed silica (FS), which has a high specific surface area (~150 m²/g), by using a previously described sol-gel process to introduce nanoscale roughness to the surface of the plastic mold, 11,12 as shown in Figure 1B-ii. On thermoplastics, the FS physically adsorbs to the plastic since the solvent temporarily plasticizes the surface and makes it tacky. 13 After the solvent evaporates, the FS remains adhered to the mold surface, even though the polymer is no longer tacky. Although we started our studies with PMMA, many plastics could be coated by using this process. Glass or metal surfaces could also be coated, although the adhesion between the FS and the mold surface was weak. After coating the FS on the mold, we rested the mold on a target substrate with the engraved side facing the substrate to form a pattern. LM was injected into the inlet of the microchannel. After lifting off the mold, the LM adhered to the substrate but not the microchannel due to the rough coating on the walls of the mold (Figure 1B-iii,iv). Even though the surface tension of the liquid metal is very high, the oxide layer that forms spontaneously on these metals adheres to the substrate. The oxide layer is also strong enough to preserve the molded shape of the LM.14 Consequently, the LM pattern retains its injected geometry even after removal of the mold.

Without the coating layer on the mold, the LM pattern does not release cleanly from the mold surface during separation (Figure 1C), which has been observed previously during transfer-printing of liquid metal. 15 The LM patterns printed by using the coated mold have a highly reproducible

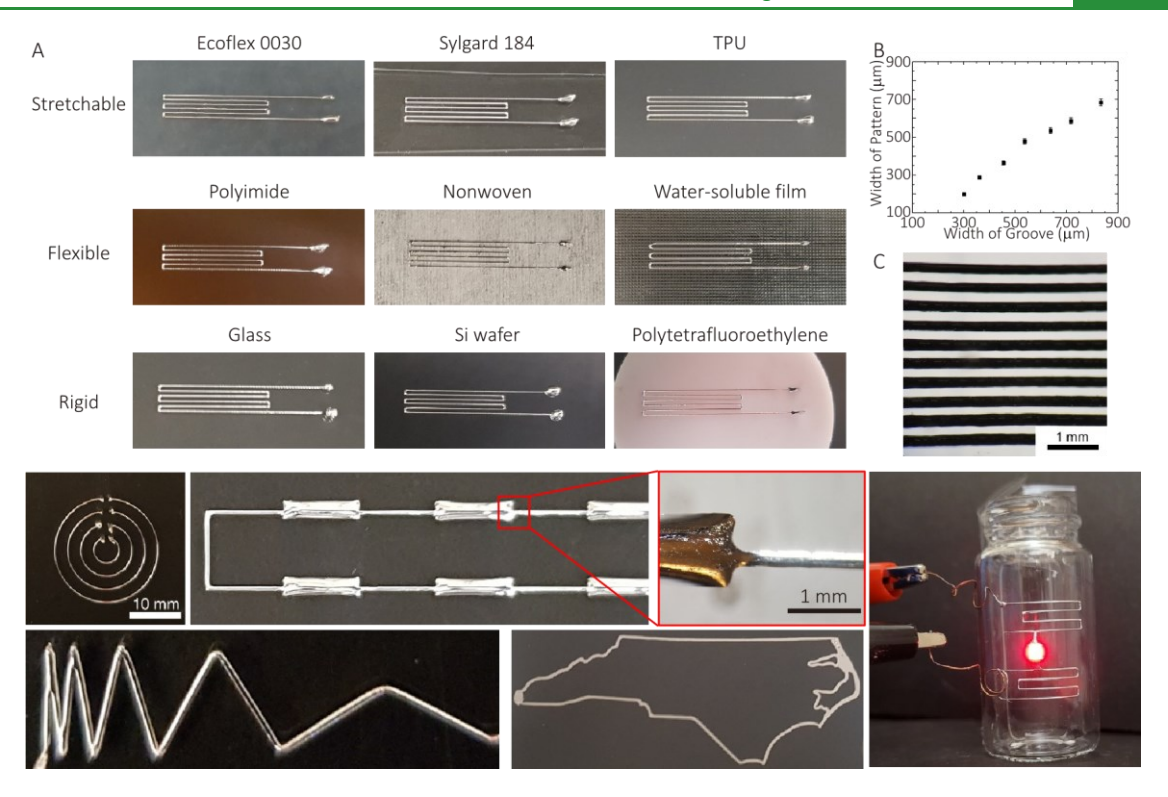


Figure 3. Various patterns of LM formed by injection molding with substrate independence. (A) Strain gauge-shaped LM pattern on various substrates. (B) Relationship between the width of the microchannel and the width of the pattern. (C) Optical image of the patterned liquid metal. (D–G) Various liquid metal patterns. (D) Concentric patterns. (E) Two different widths in the same circuit. (F) Various angles. (G) Outline of the state of North Carolina. (H) Liquid metal pattern on a curved surface (κ = 0.36 mm⁻¹).

geometry. We quantified the reproducibility by measuring the electrical resistance of injection-molded LM circuits. The small standard deviation, as shown by the "bars" on the data from six printed patterns, shows reproducibility. The resistance is in agreement with the theoretical resistance dictated by the geometry of the microchannel (Figure 1D). In contrast, the average resistance and standard deviation of the liquid metal pattern from the uncoated mold is larger, which means it is neither accurately replicating the mold shape nor precise (i.e., repeatable), as shown in Figure 1E,F.

We sought to evaluate the morphology of the surface of the silica-coated mold by varying the ratio of a good solvent to a poor solvent for the polymeric mold. We reasoned that good solvents would favor making the surface of the mold tacky if used in the right proportion with a bad solvent but could also dissolve the mold if used at unnecessarily high concentrations. For example, dichloromethane (DCM) is a good solvent, and isopropanol (IPA) is a poor solvent for PMMA. We chose these because the FS could be dispersed in both solvents. As shown in Figure 2A, the FS particles just rest on the polymer surface when coated from a poor solvent. The coating prevents the LM from adhering to the surface but gets removed completely after bath sonication for 5 min in water. Meanwhile, a good solvent, such as DCM or toluene, dissolves the mold, leaving a porous surface. We settled on DCM after finding that toluene, one of the best solvents for PMMA dissolved the PMMA too quickly and left

the surface hazy. A robust coating forms by using a mixture of good and poor solvent. As shown in Figure 2B, the FS particles stuck to the surface of the polymeric mold. The liquid metal did not adhere to the FS-treated surface. Such surfaces are sometimes called "metallophobic" in analogy to the term "hydrophobicity", but "metallophobic" is nevertheless a bit of a misnomer because it is really the oxideand not the metalthat promotes adhesion with surfaces; 16 thus, we simply call the coatings "nonstick". The thin FS coating layer itself does not change the optical transparency of the polymer. However, dissolution of the surface can cause the optical transparency of the PMMA to change depending on the ratio of good solvent to poor solvent. We conducted experiments to empirically find the optimized ratio of good to poor solvent from 1:1 to 1:5, and the ratio (1:3) was found to work best.

We evaluated the coating on various thermoplastics to demonstrate its versatility. As a control, we applied the FS coating to only the right half of a plastic mold by immersing it partially into the coating solution. To test if liquid metal adheres to the surface, we advanced and receded a droplet of EGaIn against each part. While receding the droplet, metal residue remains on the uncoated portions due to pinning of the oxide to the uncoated surface (Figure 2C). In contrast, the

liquid metal droplets receded completely from the coated surfaces in all cases (Figure 2C), which is evidence that the

oxide does not adhere due to the surface roughness of the substrate.

Fourier transform infrared spectroscopy in attenuated total reflection mode (FT-IR ATR) confirms the presence of the FS on the surface. The spectrum of the FS-coated surface indicates stronger Si-O stretching intensity at 1100 cm⁻¹, which is one of the representative peaks of the FS¹⁷ (see black and red spectrum in Figure 2D). Bath sonication removes the weakly adhered FS (Figure 2A), thereby lowering the intensity at 1100 cm⁻¹ (magenta spectrum, Figure 2D). To illustrate the importance of making the surface tacky to achieve a robust coating, we attempted to coat poly(ethylene) (PE) since it does not dissolve in the solvents used here. Consequently, after sonication of the FScoated PE in a water-containing bath sonicator for 5 min, the FS coating detached completely. Although the FS does not strongly adsorb to the PE surface, we were able to advance and recede the liquid metal on the treated surfaces at least 100 times without adhesion of the oxidecoated liquid metal. This result implies that the adhesion between the FS and the oxide on the liquid metal was weaker than the adhesion between the FS and the substrate. When the FS was robustly coated (blue spectrum, Figure 2D), the intensity of the Si-O stretching signal associated with the FS did not change after treating the substrate with sonication.

In addition to treating thermoplastics, some elastomers, like thermoplastic polyurethane (TPU), poly[styrene-b-(ethyleneco-butylene)-b-styrene] (SEBS), can be treated (Figure 2C). These materials are attractive because they can be deformed elastically at room temperature. Moreover, the surface does not adhere to the oxide-coated metal even during large uniaxial strain (400%, Figure 2E). Likewise, coated PMMA retains its nonstick nature after a thermoforming process in which the PMMA gets heated, deformed, and then cooled to change its shape (Figure 2F). The deformation does not cause FS delamination, and the coating continues to prevent adhesion of the liquid metal on those deformed surfaces.

As the liquid metal easily adheres to most surfaces regardless of their chemical composition, 16 the injection printing of the liquid metal can be done on most surfaces. As shown in Figure 3A, we injection-molded LM to the shape of a strain gauge on the elastomer to show the versatility of the process. However, the line width of the patterned liquid metal was always narrower than the width of the microchannel (Figure 3B). We attribute this decrease to the cross-sectional geometry of the channel, which prevents the high-tension metal from filling sharp corners at the edges. Indeed, confocal microscopy images show that the cross section shape of the injected liquid metal is semicircular, regardless of the cross-sectional geometry of the mold. Comparison of the cross section of the mold and liquid metal suggest that the liquid metal does not fill the entire space in the mold (Figure S1A-C). We reason that during

injection the metal follows the path of least resistance, which is along the length of the channel rather than into the narrow recesses of the mold. The elastic modulus of the substrate also affects the width of the patterned liquid metal since soft substrates can partially deform into the microchannel as shown conceptually in Figure S1D. One drawback of this process is if the substrates were tacky (e.g., VHB tape from 3M), then it became difficult to detach the mold without smearing the metal. The finest liquid metal line that we attempted was 100 μm (Figure 3C), but this was limited by the way in which we make the mold and not the molding process itself. If one can make a smaller microchannel on the thermoplastics, then the resolution of the pattern should improve further.

Like other injection-based patterning techniques, the geometry of the microchannel should have two throughholes that serve as the inlet and outlet. Various geometries (round, multiple width, lines with angles, and the border of the state of North Carolina) of the liquid metal could be patterned if the microchannel has one inlet and one outlet, as shown in Figure 3D-G. One limitation of this technique is completely filling multiple paths, such as mesh or grid patterns, since the metal will flow along the path of least resistance and therefore leave certain paths unfilled (Figure S4). In such cases, vacuum filling can completely fill the features, but this works only if the modulus of the substrate is lower than ~300 kPa to facilitate sealing with the mold. 18 Alternatively, it may be possible to fill multiple paths by using smaller openings in the outlet to create the backpressure needed to coerce the metal to fill other pathways (not shown).

As we utilized thermoplastics, it was also possible to thermoform the mold into curved shapes, as shown in Figure 3H. After injection of the metal, an LED was attached to show electrical connectivity. Potentially, this process can be utilized for three-dimensional (3D) electronics.

LM patterns embedded in elastomers show stable electromechanical properties (see the Experimental Section). As shown in Figure 4A, the resistance increased as the LM line on the stretchable substrate elongated and simultaneously narrowed, as expected. The resistance changes proportional to the square of the strain, $\lambda = \varepsilon + 1$ where λ = elongated length/original length or stretch ratio, following Pouillet's law (inset equation in Figure 4A) since the volume of the liquid metal conserves while stretching. The initial resistance of the liquid metal line is 0.55 Ω owing to the high electrical conductivity of LM. The wires failed only when the substrate failed mechanically.

The cyclability of stretchable wiring is an important parameter for the longevity of stretchable electronics. Here, we utilized a commercial elastomer, Ecoflex 0030, as a model substrate. The elastomer is highly stretchable and elastic and has negligible mechanical hysteresis up to $\sim 300\%$ strain. It is difficult to inject liquid metal into

microchannels made up of Ecoflex as they tend to collapse. Injection molding makes it possible to create liquid metal features on Ecoflex by injecting liquid metal through a microchannel mold placed on Ecoflex and followed by lifting off the mold. Pouring additional Ecoflex over the pattern encapsulates it.

First, we strain cycled the liquid metal encapsulated elastomer to 100% of strain with two different strain rate conditions (100 or 500%/s) (Figure 4B). The resistance response was almost identical for both cases over 12k cycles and there was no change of the response owing to the superior cyclability of the LM and the substrate. The surface oxide wrinkled with strain cycling, so the shiny surface lost its luster, but the internal LM did not appear to change within the resolution of our measurements. Such wrinkling may help to avoid excess oxidation of the metal wires that could otherwise cause resistance to increase during strain cycling.

Second, the sample was strain cycled to two different strains (150 and 300%) with the same strain rate (100%/s) as shown in Figure 4C. The resistance response did not change over 6000 cycles. In both cases, the encasing elastomer eventually failed due to fatigue, but the electrical connectivity remained consistent until the elastomer failed completely.

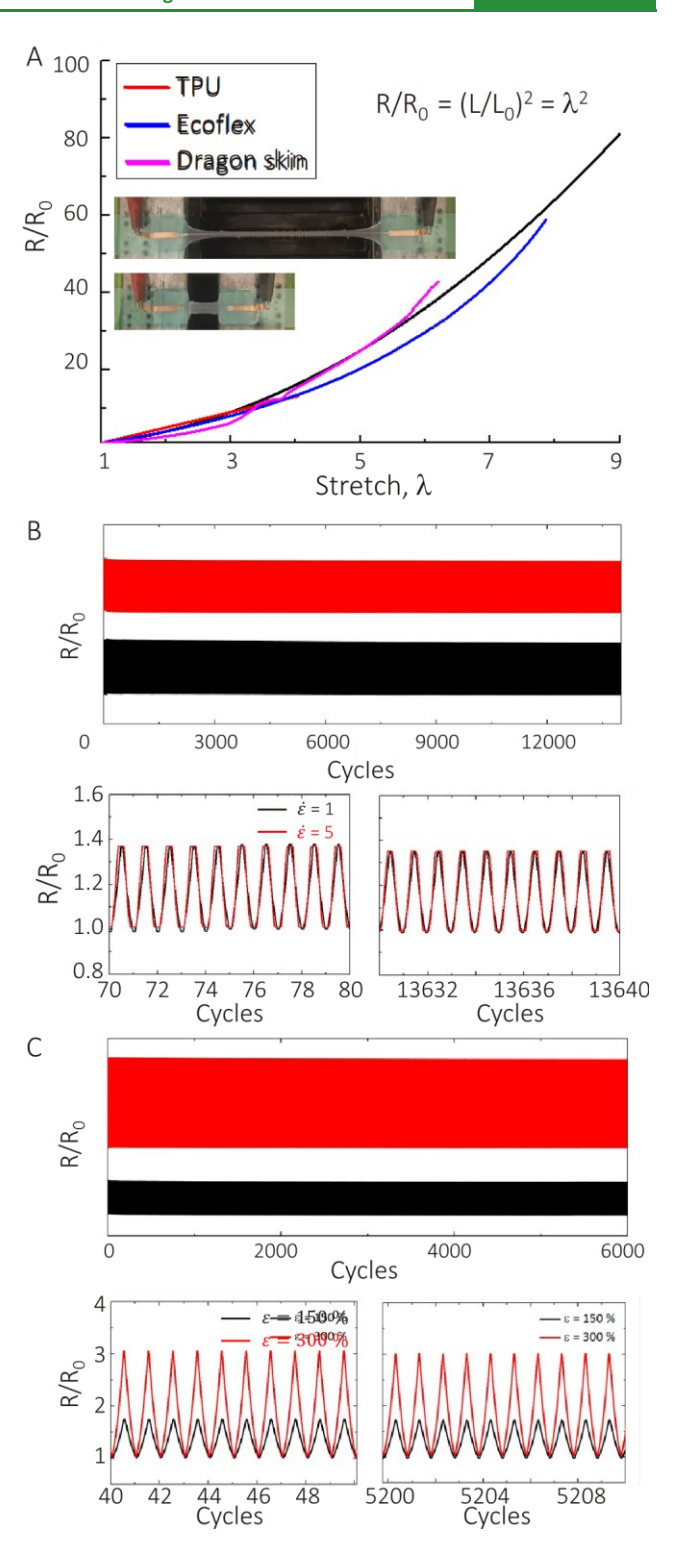


Figure 4. Electromechanical properties of the liquid metal. (A) Strain resistance plots of liquid metal wires for various stretchable substrates. (B, C) Strain cycle test of the liquid metal embedded in an elastomer (Ecoflex 0030).

Patterning processes that use injection into microchannels typically have several limitations, including (1) the incorporation of the mold in the final structure and (2) thus the need to create a new mold each time. In contrast, the injection molding process here provides an

gauge, the resistance of the liquid metal strain gauges was recorded by an electrometer (2400, Keithley). The average resistance values of the first five patterns and last five patterns were identical (\approx 1.4 as shown in Figure 5C).

Injection molding enables the linear directional flow of

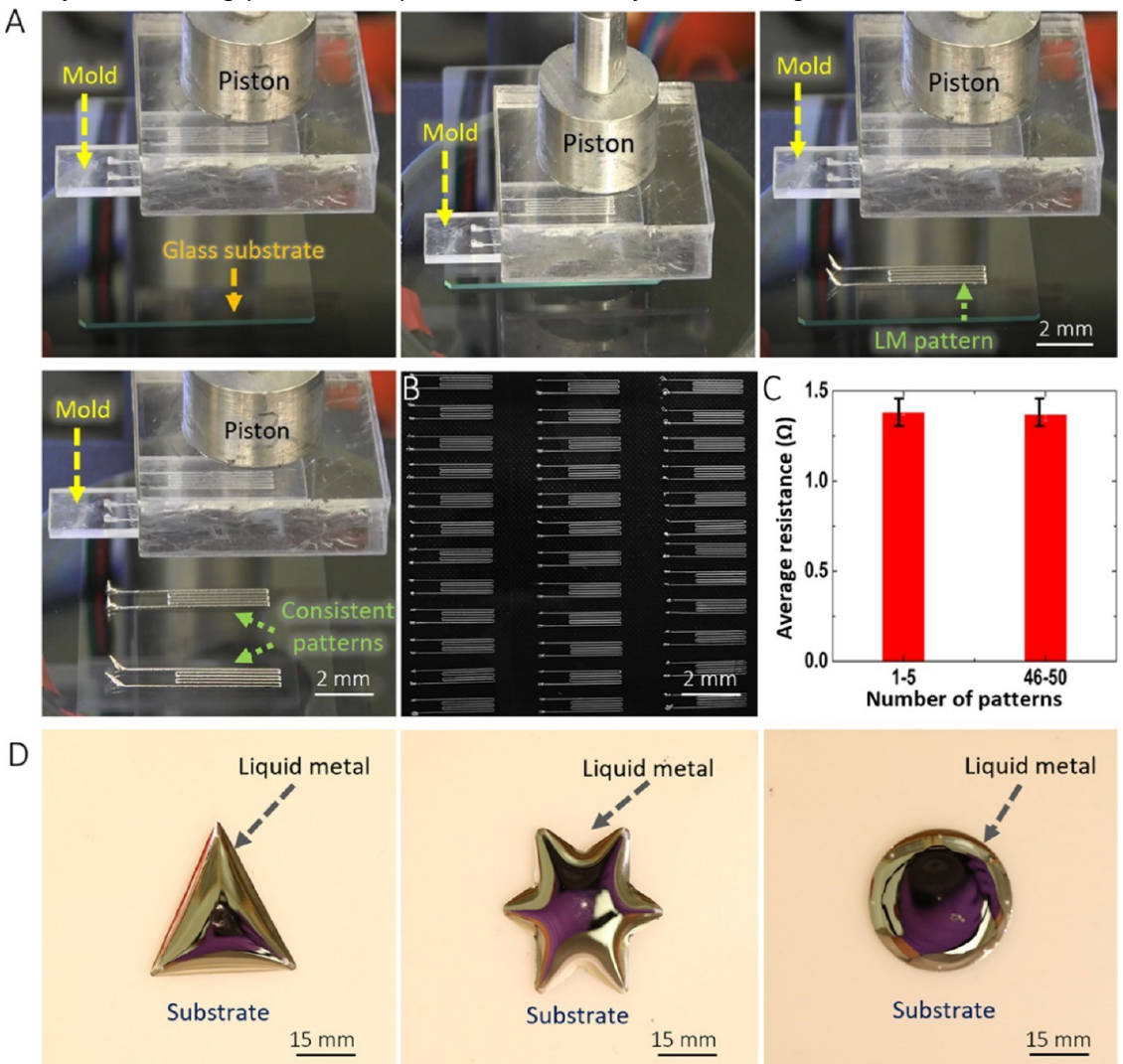


Figure 5. Repeatable printing of liquid metal (A) A piston brings mold into contact with a glass substrate prior to injection. (B) Consistent, repeatable patterns. (C) Resistance of the first five patterns is nearly identical to the resistance of the last five patterns, showing the consistency of the method. (D) Injection molding of different geometries. The purple color arises from the shiny metal surface reflecting the photographer's purple gloves.

easy way to scale up the LM patterning process and addresses limitations posed by other conventional LM patterning methods. ^{19,20} To demonstrate this advantage, we injection-molded LM circuits multiple times using the same mold (SI Videos 4, 5, and 6). The prefabricated microchannel mold was attached to a piston with the engraved part facing the substrate. Figure 5A demonstrates the steps of liquid metal injection molding: placing the mold on the substrate, injecting liquid metal, and lifting off the mold. This process was repeated 50 times using the same mold, as shown in Figure 5B. To check the consistency of the patterned strain

LM from a single inlet to a single outlet to form continuous traces. Yet, several applications require unique shapes, such as squares, which are difficult to form by other techniques. For example, liquid metals can be used to remove heat from computer chips due to the high thermal conductivity and low thermal resistance of the metal with the substrate. ^{21–28} In such applications, the LM should be dispensed over a chip in a desired shape, such as a square or rectangle, to transfer heat from the chip/die (heat source) to a heat sink that can be placed on top of the LM. It is possible to use injection molding to form such shapes composed of liquid.

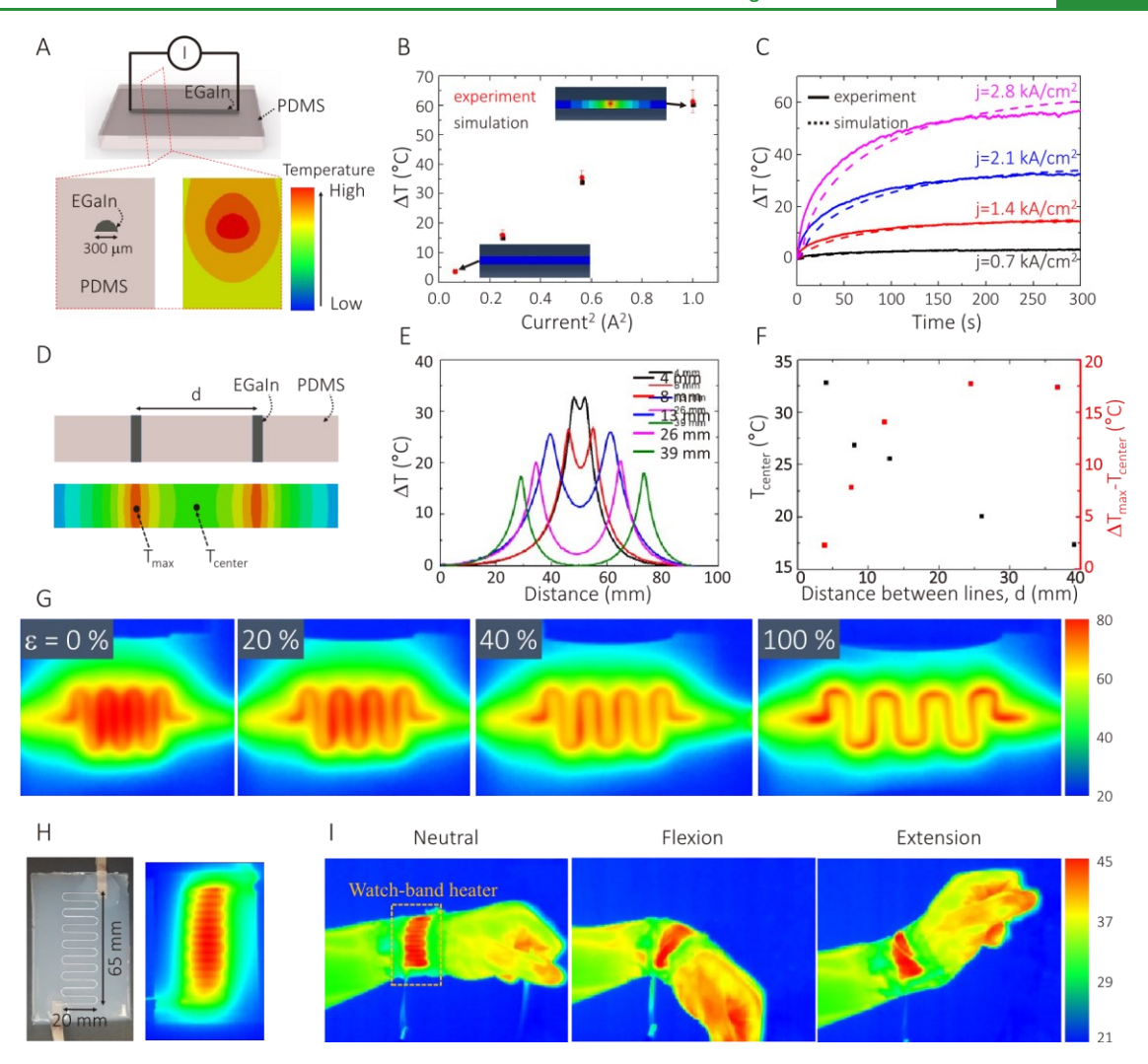


Figure 6. Joule heating using liquid metal patterned by injection molding and embedded in elastomers (PDMS, TPU). (A) A schematic diagram for the Joule heating experiment. The cross-sectional temperature distribution is presented (FEM simulation). (B) A plot of the temperature change versus current squared at steady state (time = 300 s). Red dots are experimental data, and black dots are based on the FEM simulation. (C) A transient plot of the temperature while applying current. Solid lines are experimental data, and dashed lines are based on the FEM simulation. (D) A schematic for Joule heating experiment with two liquid metal lines. (E) A plot demonstrating variation in temperature of the surface of the Joule heater (relative to room temperature) for various d values (see legend). $\Delta T = T - T_{ambient}$. (F) Black data shows T_{center} , and red data shows the $T_{max} - T_{center}$ for different d values. (G) Thermal imaging of the soft heater while stretching. (H) An optical image of the soft heater and thermal imaging with applying 0.5 A. (I) The wearable soft heater attached to the wrist worked without failure under flexion and extension.

In general, the aspect ratio (height/width) of LM features is limited to ≤1 due to the effects of surface tension (e.g., Figure S1). However, we were able to inadvertently create tall cylindrical features at the vertically oriented inlet and outlet holes (Figure 5A), which suggests that there may be clever ways to make higher aspect features by using molds that coerce the fluid to move along vertical paths in the mold. As shown in Figure S2, molds with one injection hole and multiple tiny vents can be used to form low-aspect-ratio features such as squares or circles (SI Video 7). While it is possible to form shapes such as triangles, it is apparent from the optical reflections from the surface of the metal that the cross sections of the shapes in Figure 5D have curvature.

To demonstrate the applications of these liquid metal patterns, we used them for Joule heating and electroadhesion. $^{29-34}$ To demonstrate the Joule heater, we injection-molded the LM on PDMS (Sylgard 184) and encapsulated it by pouring and curing additional PDMS as shown in Figure 6A. The width of the embedded liquid metal was $\sim\!300~\mu\text{m}$ with a semicircular cross section. The temperature of the PDMS surface was detected with a thermal imaging camera (SC300-Series, FLIR). As expected, the heat generated and thus, steady state temperature is proportional to current squared (Figure 6B). The time to reach steady state was about 3 min, regardless of the applied current (Figure 6C). Finite element method (FEM)

simulation fits the measured temperature well (Figure 6B,C). We were able to apply the current density up to \sim 5 kA/cm² (1.75 A for this geometry) without any failure. Above

to be 2.3, 7.86, 14.1, 17, and 17 $^{\circ}$ C when the distance between the lines was 4, 8, 13, 26, and 39 mm, respectively, as shown in Figure 6E,F.

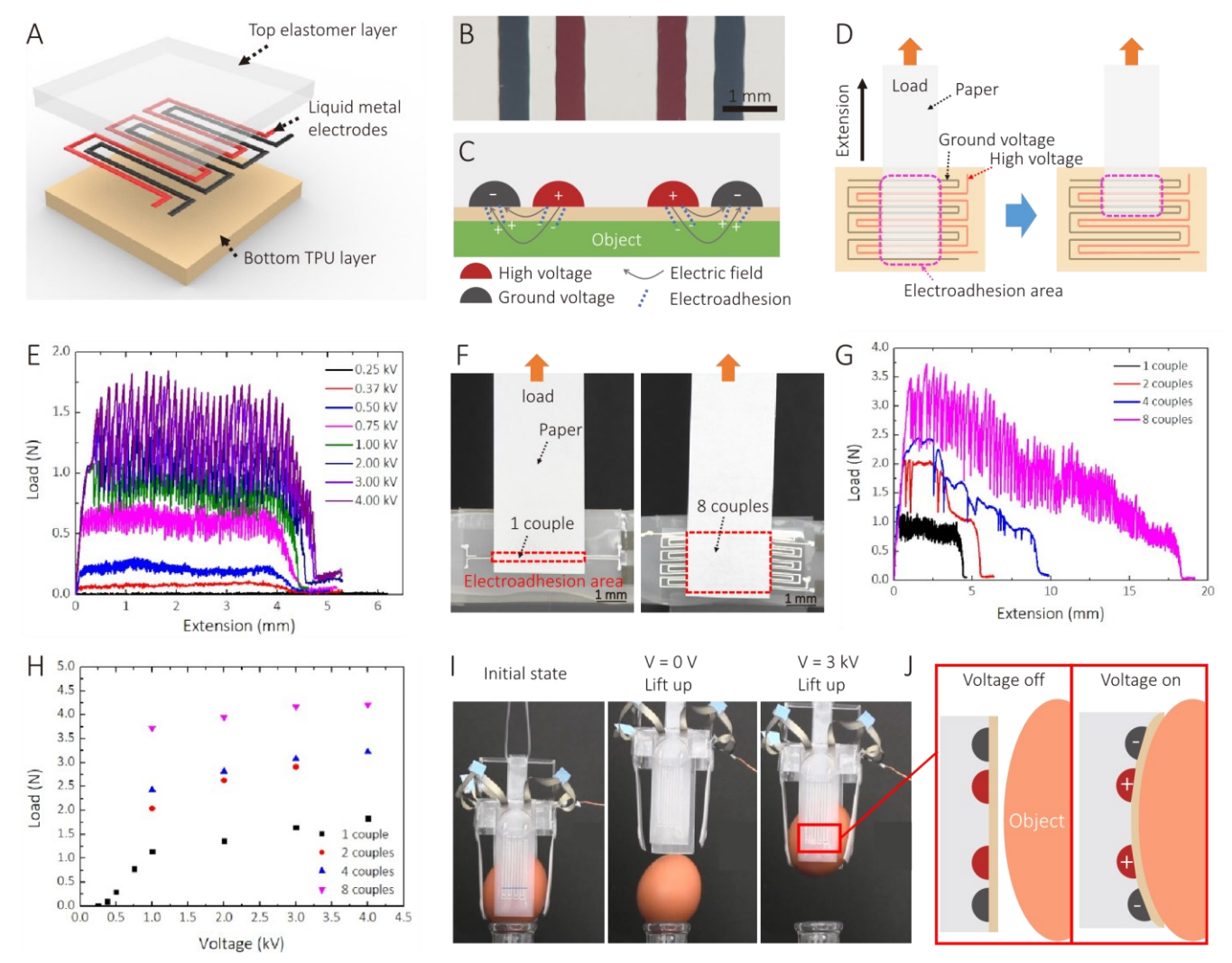


Figure 7. Electroadhesion soft gripper utilizing liquid metal electrodes formed by injection molding. (A) The structure of the electroadhesion device. (B) Optical image of the liquid metal electrodes. One electrode was colored red for visualization. (C) Schematic diagram for the electroadhesion mechanism. (D) Schematic diagram for the shear force measurement. (E) Extension—load curves for one LM electrode pair (40 mm long, 0.8 mm wide) with various voltages. (F) Optical image of the shear force measurement with different numbers of electrode couples. (G) Extension—load curves for various couples with 1 kV. (H) Load increases as the applied voltage and the number of couples increase. (I, J) Gripper demonstration. Without voltage, the gripper cannot grab the egg. With 3 kV, the gripper holds the egg.

5 kA/cm², the embedded liquid metal line disconnected within a few minutes, presumably due to either the thermal expansion of the surrounding elastomer or electromigration of the metal (Figure S3). We were not able to track the temperature of the LM Joule heater beyond the upper limit of the thermal imaging camera (150 °C), but the simulated temperature at 5 kA/cm² was 205 °C at steady state.

We quantified the minimum distance between the liquid metal lines to generate a uniform temperature field over an area by multiple liquid metal lines (Figure 6D). The difference between the maximum temperature (T_{max}) and temperature (T_{center}) between two LM lines was measured

Employing a gap of 4 mm between lines, we fabricated a wearable soft heater that could potentially be applicable for thermal therapy (Figure 6G). The soft, highly stretchable heater was attached to the wrist, as shown in Figure 6H,I. The temperature of the heater was controlled to 40–45 °C, which is appropriate for thermotherapy applications. The Joule heater worked robustly under various deformation modes, such as extension or flexion of the wrist.

As a second application, we created electroadhesive devices. Electroadhesion is the adhesive force generated by applying electric fields emanating from a surface in contact with a target object. Electroadhesion helps to handle soft

and fragile objects using lightweight and high-compliance electrodes.35-41 As shown in Figure 7A, two interdigitated electrodes were printed on 40 μm thick TPU and encapsulated with Ecoflex 0030. We applied a high voltage (up to 4 kV, 40 V/ μ m) between the two interdigitated electrodes. The distance between the electrodes is about 400 μ m (Figure 7B). Applying a high voltage creates E-fields that polarize the object, generating an electrostatic force between the electrodes and the polarized object (Figure 7C). A 25 mm wide strip of paper was pulled by shear while measuring the force utilizing a tensile tester (Instron 5943) (Figure 7D). The shear force is the summation of the electroadhesion shear force and the friction force, the latter of which depends on the materials. For example, if glass was to be used instead of paper, the friction force would dominate and there would be no noticeable difference between the force with and without the E-field. Paper is rough and therefore makes poor contact with silicone. Thus, the intrinsic low friction between the substrate and the elastomer makes it possible to measure electroadhesive force (Figure 7E). In our previous work, we observed a shear force to increase linearly with voltage, but in that work⁴² we used silicones that were less tacky than the thermoplastic urethanes used here; thus, the measured electroadhesion here is noisy due to stick-slip motion. As shown in Figure 7E, the shear force increases as the voltage increases. The maximum force measured for one electrode (40 mm long, 0.8 mm wide) couple was about 1.7 N at 4 kV. The device could hold 8 times its own mass (50 g). The shear force increases as the electroadhesion area increases (Figure 7F-H). As illustrated in Figure 7D,F, the electroadhesion area decreases as the paper slides past the electrodes, so the shear force also decreases (Figure 7G). To summarize, the shear force increases as the applied voltage and the number of electrodes increase (Figure 7H).

Utilizing four electroadhesive devices, we grabbed and manipulated an egg (\sim 60 g). As shown in Figure 7I, the gripper does not grab the egg without applying voltage, as there is insufficient adhesion force between the rough surface of the egg and the device (see Figure 7E). Applying 3 kV to the liquid metal electrodes allowed the gripper to manipulate the egg (SI Video 8 and Figure 7J). One appeal of the gripper is the weak normal force. As the normal force is one or two orders weaker than the shear force, the gripper just gently grabs the object, and there is no threat to break it. Since the electroadhesive soft gripper utilizes negligible current (less than μ A) there was no apparent damage to the metal or sample during the experiments.



CONCLUSIONS

We report the injection molding of gallium-based liquid metal patterns on arbitrary substrates. It is possible to form patterns by injecting liquid metal into a mold placed temporarily against a target substrate. A coating of fumed silica (FS) on the walls of the mold makes it possible to remove the mold while leaving only LM on the substrate and not on the mold. The native oxide on the LM preserves the shape of the structure in the absence of the mold.

Liquid metal injection molding has several advantages compared to other patterning methods. (1) The LM pattern is highly reproducible and scalable. (2) The LM patterning could be done on most substrates except for ones in which the LM does not adhere (e.g., rough surfaces) or sticky substrates that adhere to the mold. (3) LM can be patterned on lowmodulus substrates that would normally "collapse" when used as microchannels. (4) Only a single mold needs to be created since it can be reused many times. (5) It produces exposed metal surfaces, which are useful for making connections to components (cf. Figure 1a) or for encasing liquid metal in diverse materials. (6) Liquid metal injection molding can form a variety of shapes including squares, triangles, and circles.

Downsides of this approach include: (1) The need for a high-resolution microchannel mold, although there are a variety of ways to create such molds such as the laser engraving used here. (2) The need for a stable FS coating solution for a uniform coating on walls of microchannel mold. We found this works best on thermoplastic molds that can be rendered temporarily tacky using a solvent to help promote adhesion with the FS. (3) Design/pattern limitations: LM will flow along the path of least resistance (Figure S4). Thus, injection molding does not work well if there are multiple paths for the metal.

To demonstrate its versatility, we injected LM into various geometries on a variety of substrates, including stretchable substrates. The resistance follows Pouilet's law during strain cycling. The metal did not fail until the embedding matrix failed, thereby showing high cyclability under various deformation conditions. We also demonstrated (1) a wearable Joule heater that can conformally attach to the body for thermotherapy applications and (2) a soft gripper using electroadhesion forces. In principle, this injection molding can also be extended to other applications, such as implantable, transient electronics, stretchable printed circuit boards, electronic skins, and soft robotics.

EXPERIMENTAL SECTION

Materials. Eutectic gallium-indium alloy (EGaIn) was purchased from Indium Corporation. Fumed silica (Aerosil 150, Evonik Industries) was purchased from Evonik. Isopropyl alcohol (IPA) and acetone were purchased from VWR. Toluene and

tetrahydrofuran (THF) were purchased from Sigma-Aldrich. Thermoplastics: Cast poly(methyl methacrylate) sheet (8560K172) was purchased from McMaster, and polyethylene was purchased from Sigma-Aldrich Thermoplastic elastomers: various grades of triblock copolymer of styrene-ethylene-butylene-styrene (SEBS) were purchased from Kraton (G1650). Thermoplastic polyurethane (TPU) was kindly provided by Murata Electronics. Elastomers: Ecoflex 0030 was purchased from Smooth-On, Inc. Sylgard 184 was purchased from Dow Corning. A water-soluble film that has a 35 μ m thickness was purchased from Amazon. Unless otherwise specified, the chemicals used in the current work were used without further purification.

Injection-Printing Process of the Liquid Metal. Preparation of Microchannel on Thermoplastics. Microchannels were ablated with a commercial laser writing system (VLS 3.50, Universal Laser Systems) with a 40 W CO₂ laser operating at 10.6 μ m. The geometry of the microchannels depends on the speed and power of the head. Typically, 30% power and 20% speed were used to achieve a channel of 300 μ m width. Poly(methyl methacrylate) sheets were generally used as a mold. CorelDRAW (Corel) was utilized to draw the patterns used by the laser cutter.

Coating Process of the Fumed Silica on the Thermoplastics. A fumed silica (1% w/v) was freshly dispersed in the appropriate organic solvent determined empirically. As the fumed silica is hydrophilic, polar organic solvents were used. For PMMA, a 1:1 mixture of good solvent (DCM) and poor solvent (IPA) was typically used. After mixing the fumed silica and the solvent, vortex mixing was applied for 30 s to improve the dispersity of the fumed silica. The thermoplastics were immersed in the mixture for 30 s; then, they were dried completely using compressed air.

Injection Molding of the Liquid Metal. After coating the FS on the thermoplastic mold, the mold was placed on a substrate with the engraved microchannel side down. The liquid metal was injected into the inlet of the microchannel and came out of the outlet while the microchannel was filled with the liquid metal. After the mold was carefully lifted off, the liquid metal pattern that has the same geometry as the microchannel is left on the substrate.

Soft, Wearable Heater Utilizing Joule Heating of the Liquid Metal. A 40 mm long, 300 μm diameter hemispherical liquid metal was injection-printed on 500 μ m thick solid PDMS, and then an additional 1 mm thick PDMS was cured on it after adding a strip of conductive nylon tape (3961, ada fruit) at each end. Various levels of current (0.25-1.75, 0.25 A of interspacing) were applied at least for 5 min. The generated thermal field was observed by a thermal imaging camera (SC300-series, FLIR). For the watch-band-type soft heater, a serpentine-shaped liquid metal was inject-printed on 40 μ m thick TPU, and then 1 mm thick ecoflex 0030 was cured on it after adding a strip of conductive nylon tape. To enhance the adhesion between the elastomer and TPU, 3-(trimethoxysilyI) propyl methacrylate was coated by using a vacuum process before curing the Ecoflex 0030. An electrothermal analysis was carried out to calculate the thermal field of the Joule heating of the liquid metal by using a commercial finite element method (FEM) software (Abaqus 6.13).

Soft Gripper Utilizing Electroadhesion of the Liquid Metal Electrodes. . Two parallel, interdigitated liquid metals (see Figure 6A) were patterned on 40 μ m thick TPU, and then, 1 mm of Ecoflex was cured on it after adding a strip of conductive nylon tape at the terminals. Before the curing step, TPU was treated as described in the previous paragraph. The shear force between a paper and the

electroadhesion device was recorded by a tensile test machine (5934, Instron) while pulling the paper and applying a voltage up to 4 kV by using a high-voltage amplifier to the electroadhesion device. To fabricate the soft gripper, four electroadhesion devices were attached to a structure to have a 5 cm distance. To lift an egg (\sim 56 g), 3 kV of voltage was applied to each electroadhesion device.

Electromechanical Characterization of the Liquid Metal Embedded in Elastomers. A 20 mm long, 300 μm diameter hemispherical liquid metal was inject-printed on the 1 mm thick, dog-bone shaped, stretchable, soft substrates (Ecoflex 0030, dragonskin 0010, and TPU), and then an additional 1 mm thick elastomer was cured on it after adding a strip of conductive nylon tape (3961, Ada fruit) at each end. The average contact resistance between the nylon tape and the liquid metal wire was calculated as 0.48 Ω by utilizing the transmission line method. The resistance of the liquid metal wire in Figure 4 is subtraction from the whole resistance to the contact resistance. 200 μm thick PET was attached to the grip section, then the PET was grabbed by a homemade uniaxial stretcher. The resistance of the liquid metal wire was recorded with two electrode probes by using an electrometer (2400, Keithley). The rate of the deformation was set from 100 to 500%/s.

Characterization of the FS-Coated PMMA. A PMMA substrate with dimensions of 8 \times 8 \times 1.5 mm³ (width \times length \times thickness) was cut by using a laser writing machine; then, the plastic was coated with the fumed silica as described in the previous paragraph. The morphology of the samples was observed by scanning electron microscopy (SEM) (Verios 460L, FEI). Fourier–transform infrared (FT-IR) spectra in the 600–4000 cm $^{-1}$ wavenumber range and a step of 4 cm $^{-1}$ were recorded using a Nicolet iS 9 FT–IR spectrometer (Thermo Scientific) operating in the attenuated total reflection (ATR) mode. UV–vis spectra in the visible range (400–700 nm) were recorded by using a UV–vis spectrometer.



ASSOCIATED CONTENT

* Supporting Information

The Supporting Information is available free of charge at https://pubs.acs.org/doi/10.1021/acsami.3c16692.

Confocal microscopy images, liquid metal patterning with complex-shaped molds, LM wire failure experiments with high current density, and injection molding of the liquid metal with molds that have multiple

pathways (PDF) Mold
fabrication (MP4)
Fumed silica coating (MP4)
Injection mold lift-off (MP4) Single
pattern (MP4)
Reproducible patterning of LM (MP4)
Large-scale patterning of liquid metals (MP4)
Liquid metal films (MP4)
Electroadhesive gripper (MP4)

25 mm Al foil 40 g at 4 kV drop after 1 s (MP4)



AUTHOR INFORMATION

Corresponding Author

Michael D. Dickey – Department of Chemical and Biomolecular Engineering, North Carolina State University,

Raleigh, North Carolina 27695, United States; orcid.org/

0000-0003-1251-1871; Email: mddickey@ncsu.edu

Authors

Jinwoo Ma – Department of Chemical and Biomolecular Engineering, North Carolina State University, Raleigh, North

Carolina 27695, United States; o orcid.org/0000-0001-5140-2972

Dhwanil P. Vaghani – Department of Chemical and Biomolecular Engineering, North Carolina State University,

Raleigh, North Carolina 27695, United States

Sooik Im – Department of Chemical and Biomolecular Engineering, North Carolina State University, Raleigh, North

Carolina 27695, United States

Minsik Kong – *Department of Chemical and Biomolecular*

Engineering, North Carolina State University, Raleigh, North

Carolina 27695, United States

Mohammad Shamsi – Department of Chemical and Biomolecular Engineering, North Carolina State University,

Raleigh, North Carolina 27695, United States
Shuzhen Wei – Wilson College of Textiles, NC State
University, Raleigh, North Carolina 27695, United
States

Man Hou Vong – Department of Chemical and Biomolecular

Engineering, North Carolina State University, Raleigh, North

Carolina 27695, United States

Complete contact information is available at: https://pubs.acs.org/10.1021/acsami.3c16692

Author Contributions

M.D.D. and J.M. conceived the project and directed it. J.M. and D.P.V. performed a majority of the sample preparation and experiments. S.I. and M.S. characterized the mechano-

electrical properties of the pattern and helped SEM experiments. M.K. performed the advancing and receding of the liquid metal. J.M. and S.W. performed electroadhesion experiments utilizing high voltage. M.H.V. performed experiments on injection molding of the complex-shaped molds. J.M., D.P.V., and M.D.D. wrote the manuscript with inputs from all authors.

Notes

The authors declare no competing financial interest.



ACKNOWLEDGMENTS

J.M. is thankful to Dr. Younghoon Lee (Gachon University) for assisting with the fabrication of the electroadhesion devices. J.M. and M.D.D. are thankful to Prof. Tushar Ghosh (NC State University) for access to his laboratory. M.D.D. is grateful for support from the National Science Foundation Division of Civil, Mechanical, and Manufacturing Innovation grant 2032409.



REFERENCES

- (1) Chandler, J. E.; Messer, H. H.; Ellender, G. Cytotoxicity of Gallium and Indium Ions Compared with Mercuric Ion. *J. Dent. Res.* 1994, *73* (9), 1554–1559.
- (2) Ma, J.; Krisnadi, F.; Vong, M. H.; Kong, M.; Awartani, O. M.; Dickey, M. D. Shaping a Soft Future: Patterning Liquid Metals. *Adv. Mater.* 2023, *35* (19), No. 2205196.
- (3) Dickey, M. D.; Chiechi, R. C.; Larsen, R. J.; Weiss, E. A.; Weitz, D. A.; Whitesides, G. M. Eutectic Gallium-Indium (EGaln): A Liquid Metal Alloy for the Formation of Stable Structures in Microchannels at Room Temperature. *Adv. Funct. Mater.* 2008, *18* (7), 1097–1104. (4) Cademartiri, L.; Thuo, M. M.; Nijhuis, C. A.; Reus, W. F.; Tricard, S.; Barber, J. R.; Sodhi, R. N. S.; Brodersen, P.; Kim, C.; Chiechi, R. C.; Whitesides, G. M. The Electrical Resistance of AgTSS(CH2)n-1CH3//Ga2O3/EGaln Tunneling Junctions. *J. Phys. Chem. C* 2012, *116*, 10848–10860.
- (5) Catic, I. J. Cavity Temperaturean Important Parameter in the Injection Molding Process. *Polym. Eng. Sci.* 1979, *19* (13), 893–899.
- (6) Cheng, S.; Wu, Z. Microfluidic Electronics. *Lab. Chip* 2012, *12*(16), 2782–2791.
- (7) Gol, B.; Kurdzinski, M. E.; Tovar-Lopez, F. J.; Petersen, P.; Mitchell, A.; Khoshmanesh, K. Hydrodynamic Directional Control of Liquid Metal Droplets within a Microfluidic Flow Focusing System. *Appl. Phys. Lett.* 2016, *108* (16), No. 164101.
- (8) Fassler, A.; Majidi, C. Soft-Matter Capacitors and Inductors for Hyperelastic Strain Sensing and Stretchable Electronics. *Smart Mater. Struct.* 2013, *22* (5), No. 055023.

- (9) Kim, H.-J.; Son, C.; Ziaie, B. A Multiaxial Stretchable Interconnect Using Liquid-Alloy-Filled Elastomeric Microchannels. *Appl. Phys. Lett.* 2008, *92* (1), No. 011904.
- (10) So, J.-H.; Dickey, M. D. Inherently Aligned Microfluidic Electrodes Composed of Liquid Metal. *Lab. Chip* 2011, *11* (5), 905–911.
- (11) Schaefer, D. W.; Hurd, A. Growth and Structure of Combustion Aerosols: Fumed Silica. *Aerosol Sci. Technol.* 1990, *12*, 876–890.
- (12) Deng, X.; Mammen, L.; Butt, H.-J.; Vollmer, D. Candle Soot as a Template for a Transparent Robust Superamphiphobic Coating. *Science* 2012, *335* (6064), 67–70.
- (13) Ma, J.; Bharambe, V. T.; Persson, K. A.; Bachmann, A. L.; Joshipura, I. D.; Kim, J.; Oh, K. H.; Patrick, J. F.; Adams, J. J.; Dickey, M. D. Metallophobic Coatings to Enable Shape Reconfigurable Liquid Metal Inside 3D Printed Plastics. *ACS Appl. Mater. Interfaces* 2021, *13*, 12709–12718.
- (14) Dickey, M. D. Emerging Applications of Liquid Metals Featuring Surface Oxides. *ACS Appl. Mater. Interfaces* 2014, *6* (21), 18369–18379.
- (15) Zhang, S.; Wang, B.; Jiang, J.; Wu, K.; Guo, C. F.; Wu, Z. HighFidelity Conformal Printing of 3D Liquid Alloy Circuits for Soft Electronics. *ACS Appl. Mater. Interfaces* 2019, *11*, 7148–7156.
- (16) Joshipura, I. D.; Persson, K. A.; Truong, V. K.; Oh, J.-H.; Kong, M.; Vong, M. H.; Ni, C.; Alsafatwi, M.; Parekh, D. P.; Zhao, H.; Dickey, M. D. Are Contact Angle Measurements Useful for OxideCoated Liquid Metals? *Langmuir* 2021, *37* (37), 10914–10923.
- (17) Agarwal, A.; Tomozawa, M. Correlation of Silica Glass Properties with the Infrared Spectra. *J. Non-Cryst. Solids* 1997, *209*, 166–174.
- (18) Lin, Y.; Gordon, O.; Khan, M. R.; Vasquez, N.; Genzer, J.; Dickey, M. D. Vacuum Filling of Complex Microchannels with Liquid Metal. *Lab. Chip* 2017, *17* (18), 3043–3050.
- (19) Joshipura, I. D.; Ayers, H. R.; Majidi, C.; D Dickey, M. Methods to Pattern Liquid Metals. *J. Mater. Chem. C* 2015, *3* (16), 3834–3841.
- (20) Jeong, S. H.; Hjort, K.; Wu, Z. Tape Transfer Atomization Patterning of Liquid Alloys for Microfluidic Stretchable Wireless Power Transfer. *Sci. Rep.* 2015, *5* (1), No. 8419.
- (21) Chen, S.; Deng, Z.; Liu, J. High Performance Liquid Metal Thermal Interface Materials. *Nanotechnology* 2021, *32* (9), No. 092001.
- (22) Wang, X.; Lu, C.; Rao, W. Liquid Metal-Based Thermal Interface Materials with a High Thermal Conductivity for Electronic Cooling and Bioheat-Transfer Applications. *Appl. Therm. Eng.* 2021, 192, No. 116937.
- (23) Huang, K.; Qiu, W.; Ou, M.; Liu, X.; Liao, Z.; Chu, S. An AntiLeakage Liquid Metal Thermal Interface Material. *RSC Adv.* 2020, *10* (32), 18824–18829.
- (24) Ji, Y.; Yan, H.; Xiao, X.; Xu, J.; Li, Y.; Chang, C. Excellent Thermal Performance of Gallium-Based Liquid Metal Alloy as Thermal Interface Material between Aluminum Substrates. *Appl. Therm. Eng.* 2020, *166*, No. 114649.
- (25) Zhao, L.; Liu, H.; Chen, X.; Chu, S.; Liu, H.; Lin, Z.; Li, Q.; Chu, G.; Zhang, H. Liquid Metal Nano/Micro-Channels as Thermal Interface Materials for Efficient Energy Saving. *J. Mater. Chem. C* 2018, *6* (39), 10611–10617.
- (26) Hamdan, A. M.; McLanahan, A. R.; Richards, R. F.; Richards, C. D. Characterization of a Liquid-Metal Micro Droplets

- Thermal Interface Material. Exp. Therm. Fluid Sci. 2011, 3, 1250–1254.
- (27) Wang, H.; Xing, W.; Chen, S.; Song, C.; Dickey, M. D.; Deng, T. Liquid Metal Composites with Enhanced Thermal Conductivity and Stability Using Molecular Thermal Linker. *Adv. Mater.* 2021, *33* (43), No. 2103104.
- (28) Xing, W.; Wang, H.; Chen, S.; Tao, P.; Shang, W.; Fu, B.; Song, C.; Deng, T. Gallium-Based Liquid Metal Composites with Enhanced Thermal and Electrical Performance Enabled by Structural Engineering of Filler. *Adv. Eng. Mater.* 2022, *24* (9), No. 2101678.
- (29) Wang, Y.; Yu, Z.; Mao, G.; Liu, Y.; Liu, G.; Shang, J.; Qu, S.; Chen, Q.; Li, R.-W. Printable Liquid-Metal@PDMS Stretchable Heater with High Stretchability and Dynamic Stability for Wearable Thermotherapy. *Adv. Mater. Technol.* 2019, *4* (2), No. 1800435.
- (30) Li, Y.-Q.; Zhu, W.-B.; Yu, X.-G.; Huang, P.; Fu, S.-Y.; Hu, N.; Liao, K. Multifunctional Wearable Device Based on Flexible and Conductive Carbon Sponge/Polydimethylsiloxane Composite. *ACS Appl. Mater. Interfaces* 2016, *8* (48), 33189–33196.
- (31) Jang, N.-S.; Kim, K.-H.; Ha, S.-H.; Jung, S.-H.; Lee, H. M.; Kim, J.-M. Simple Approach to High-Performance Stretchable Heaters Based on Kirigami Patterning of Conductive Paper for Wearable Thermotherapy Applications. *ACS Appl. Mater. Interfaces* 2017, *9* (23), 19612–19621.
- (32) Yang, Y.; Jiao, P. Nanomaterials and Nanotechnology for Biomedical Soft Robots. *Mater. Today Adv.* 2023, *17*, No. 100338.
- (33) Jin, Y.; Lin, Y.; Kiani, A.; Joshipura, I. D.; Ge, M.; Dickey, M. D. Materials Tactile Logic via Innervated Soft Thermochromic Elastomers. *Nat. Commun.* 2019, *10* (1), No. 4187.
- (34) Yang, J.; Nithyanandam, P.; Kanetkar, S.; Kwon, K. Y.; Ma, J.; Im, S.; Oh, J.-H.; Shamsi, M.; Wilkins, M.; Daniele, M.; Kim, T.; Nguyen, H. N.; Truong, V. K.; Dickey, M. D. Liquid Metal Coated Textiles with Autonomous Electrical Healing and Antibacterial Properties. *Adv. Mater. Technol.* 2023, *8* (14), No. 2202183.
- (35) Piskarev, Y.; Devincenti, A.; Ramachandran, V.; Bourban, P.-E.; Dickey, M. D.; Shintake, J.; Floreano, D. A Soft Gripper with Granular Jamming and Electroadhesive Properties. *Adv. Intell. Syst.* 2023, *5* (6), No. 2200409.
- (36) Shintake, J.; Cacucciolo, V.; Floreano, D.; Shea, H. Soft Robotic Grippers. *Adv. Mater.* 2018, *30* (29), No. 1707035.
- (37) Yeo, J. C.; Yap, H. K.; Xi, W.; Wang, Z.; Yeow, C.-H.; Lim, C. T. Flexible and Stretchable Strain Sensing Actuator for Wearable Soft Robotic Applications (Adv. Mater. Technol. 3/2016). *Adv. Mater. Technol.* 2016, *1* (3), No. 1600018.
- (38) Hines, L.; Petersen, K.; Lum, G. Z.; Sitti, M. Soft Actuators for Small-Scale Robotics. *Adv. Mater.* 2017, *29* (13), No. 1603483.
- (39) Argatov, I. I.; Borodich, F. M. A Macro Model for Electroadhesive Contact of a Soft Finger With a Touchscreen. *IEEE Trans. Haptics* 2020, *13* (3), 504–510.
- (40) Navas, E.; Fernández, R.; Sepúlveda, D.; Armada, M.; Gonzalez-de-Santos, P. Soft Grippers for Automatic Crop Harvesting: A Review. *Sensors* 2021, *21* (8), No. 2689.
- (41) Ruffatto, D.; Parness, A.; Spenko, M. Improving Controllable Adhesion on Both Rough and Smooth Surfaces with a Hybrid Electrostatic/Gecko-like Adhesive. *J. R. Soc., Interface* 2014, *11*, No. 20131089.
- (42) Park, S.; Shintake, J.; Piskarev, Y.; Wei, Y.; Joshipura, I.; Frey, E.; Neumann, T.; Floreano, D.; Dickey, M. D. Stretchable and Soft Electroadhesion Using Liquid-Metal Subsurface Microelectrodes. *Adv. Mater. Technol.* 2021, *6* (9), No. 2100263.